Heteroleptic NHC cycloplatinated complexes: a new approach to highly efficient blue-light emitters.

Sara Fuertes[a], Andrés J. Chueca[a], Lorenzo Arnal[a], Antonio Martín[a], Umberto Giovanella [b], Chiara Botta [b] and Violeta Sicilia[c].*

[a] Departamento de Química Inorgánica, Facultad de Ciencias, Instituto de Síntesis Química y Catálisis Homogénea (ISQCH), CSIC - Universidad de Zaragoza, Pedro Cerbuna 12, 50009, Zaragoza (Spain)

b Istituto per lo Studio delle Macromolecole, Consiglio Nazionale delle Ricerche (CNR), Via Corti 12, 20133, Milano, Italy

c Departamento de Química Inorgánica, Escuela de Ingeniería y Arquitectura de Zaragoza, Instituto de Síntesis Química y Catálisis Homogénea (ISQCH), CSIC - Universidad de Zaragoza, Campus Río Ebro, Edificio Torres Quevedo, 50018, Zaragoza (Spain).E-mail: sicilia@unizar.es

Dedicated to Professor Elena Lalinde on the occasion of her 60th birthday

ABSTRACT. New heteroleptic compounds of Pt(II) containing cyclometalated N-heterocyclic carbenes, [PtCl(R-C^C*)(PPh_3)] (R-CH^C*-κC*= 3-methyl-1-(naphthalen-2-yl)-1*H*-imidazol-2-ylidene (R-C= Naph) **1A**; 1-(4-(ethoxycarbonyl)phenyl)-3-methyl-1*H*-imidazol-2-ylidene (R = CO_2Et, **1B**) and [Pt(R-C^C*)(py)(PPh_3)]PF_6 (py = pyridine; R-C = Naph, **2A**; R = CO_2Et, **2B**), have been prepared and fully characterized. All of them were obtained as the *trans*-(C*, PPh_3) isomer in high yields. The selectivity of their synthesis has been explained in terms of the degree of transphobia (T) of pairs of ligands in *trans* positions. The X-ray diffraction studies on both,

2A and **2B**, revealed that only in **2A**, containing a C^C* with a more extended π-system, the molecules assemble themselves into head-to-tail pairs through intermolecular π···π contacts. The photophysical properties of **2A** and **2B** and those of the related compounds [Pt(NC-C^C*)(PPh_3)L]PF_6 (NC-CH^C*-κC*= 1-(4-cyanophenyl)-3-methyl-1*H*-imidazol-2-ylidene; L = pyridine (py, **2C**), 2,6-dimethylphenylisocyanide (CNXyl, **3C**) and 2-mercapto-1-methylimidazole (MMI, **4C**) have been examined to analyze the influence of the R-substituent on the R-C^C* (R-C = Naph, R = CO_2Et, CN) and that of the ancillary ligands (L) on them. Experimental data and TD-DFT calculations showed the similarity of the electronic features associated to R-C^C* (R= CN, CO_2Et) and the difference of them with respect to R-C^C* (R-C = Naph). All the compounds are very efficient blue-emitters in PMMA films under Ar atmosphere, with QY values ranging from 68% (**2B**) to 93% (**2C**). In solid state, the color of the emission changes to yellowish-orange for compounds **2A** (λ_{max} = 600 nm) and **3C** (λ_{max} = 590 nm), because of formation of aggregates through intermolecular π···π interactions. **2C** and **3C** were chosen to fabricate fully solution-processed electroluminescent devices with blue (**2C**), yellow-orange (**3C**) and white light (mixtures of **2C**:**3C**) emission from neat films of the compounds as emitting layers.

INTRODUCTION

Extensive investigations on phosphorescent transition metal complexes have been carried out in the last decade driven especially by their applicability in organic light emitting devices (OLEDs), particularly those of Ru(II), Ir(III) and Pt(II).[1-5] The efficiency in the emission of visible light is attributed to the strong spin-orbit coupling (SOC) induced by the heavy metal atom that facilitates both fast intersystem crossing (ISC) and the formally spin-forbidden triplet radiative decay, which lead to conversion rates of up to 100%.[6-8]

Currently, most blue-emitting materials with high quantum yield are based on Ir(III) as the metal ion, but the number of Pt(II) compounds is increasingly growing.[3, 9-16] Population of a high energy excited state required for an efficient blue emission upon excitation competes with the photo- or thermal population of high-lying metal dd* states, the later leading to severe geometrical distortions of the molecules which result in non-radiative deactivation and degradation via bond-breaking processes.[17] In the chemistry of Pt(II), a common approach for the design of efficient and stable blue-phosphorescent systems is the incorporation of strong field ligands to the metal coordination sphere, such as C-deprotonated imines able to act as bidentate,[18, 19] tridentate[11, 17, 20] and even tetradentate[21-24] ligands. The use of bidentate ligands has the advantage of the allowed electronic tunability of the Pt(II) complexes by varying the ancillary ligands. In this context, cyclometalated N-heterocyclic carbenes (C^C*) may surpass the high ligand field splitting capacity of the C^N-ligands, since they present two C-σ bonds. Another consequence of the presence of strong carbon-metal bonds is the robustness and/or stability of the carbene complexes which may provide long-term functional materials.[10-16, 25, 26,] Up to now, most Pt(II) compounds containing C^C* cyclometalated ligands contain β–diketonate ligands,[16, 25-34] or two equal monodentate ligands[35] to complete the coordination sphere of the platinum center, but it is a constraining factor in the design of a variety of complexes. In a previous work we reported that based on the NMR data, the trans-influence of the carbene (C*) is very high and not much different from that of the metalated C atom, in such a way that attempts to synthesize heteroleptic Pt(II) complexes containing bidentate C^C* cyclometalated ligands, [Pt(C^C*)LL'], render mixtures of the *trans*- and *cis*-(C*, L) isomers.[36] However, we concluded that if L = PPh_3 the degree of transphobia T[CAr/PPh_3)] of this pair of ligands in *trans* positions is larger than T[C*/PPh_3] and directs the selective formation of the

trans-(C*, PPh_3) isomer, in such a way that the heteroleptic complexes [PtCl(NC-C^C*)(PPh_3)] (**1C**) and [Pt(NC-C^C*)(PPh_3)L]PF_6 (L = py **2C**, CNXyl **3C**, MMI **4C**) could be selectively obtained as the trans-(C*/PPh_3) isomer, and they are the only heteroleptic C^C* cyclometalated compounds of Pt(II) reported so far.[36]

Aiming to explore the generality of this assessment we have expanded the research to the synthesis of new related compounds varying the cyclometalated NHC ligands: [Pt(R-C^C*)Cl(PPh_3)] (R-C = Naph **1A**, R = CO_2Et **1B**) and [Pt(R-C^C*)(py)(PPh_3)]PF_6 (R-C = Naph **2A**, R = CO_2Et **2B**). We have also studied the photophysical properties of the ionic compounds **2A**-**2C**, **3C** and **4C**, both, experimental and theoretically, through TD-DFT calculations, trying to compare the effect of varying either the C^C* or the L ligand on it (L = py, CNXyl, MMI). Moreover, compounds **2C** and **3C** were chosen to fabricate Organic Light Emitting Diodes (OLEDs) with blue (**2C**), yellow-orange (**3C**) and white light (mixtures of **2C**:**3C**) emission. OLEDs were fabricated by a full solution process technology with a non-doped emitting layer (EML) thanks to the good processability of the compounds. Most of the works on Pt based OLEDs deals with devices fabricated with vacuum evaporation techniques[37-39] due to the low solubility and/or poor ability of these compounds to form thin homogeneous films when deposited from solution. To the best of our knowledge, solution processed devices so far reported have been obtained with emissive layer (EML) composed by host-guest systems where the Pt emitter is blended in either polymeric or molecular hosts in order to reduce aggregation quenching processes and to increase the film homogeneity, both for molecular[40-44] and dendrimeric emitters.[45, 46] For these reasons all the devices so far reported with non-doped EML have been obtained by using vacuum processed technologies.[47, 48] On the other hand, non-doped devices offer many advantages, as the higher color stability and simpler device structure.

Moreover, for blue emitting devices, the use of blends imposes strict requirements on the host triplet energy levels, whose energy must be high enough to prevent back-transfer processes. To the best of our knowledge, the results reported in this paper represent the first example of solution processed Pt-based devices obtained with non-doped EML. With this very simple approach, by mixing two compounds at different ratios, we are able to tune the OLEDs emission from blue to yellow-orange, passing through white.

EXPERIMENTAL SECTION

General Comments. Instrumental methods used for characterization and spectroscopic studies, DFT computational details, X-ray structures, details of the preparation of PMMA films and fabrication of electroluminescent devices are contained in the Supporting Information. All chemicals were used as supplied and [{Pt(μ-Cl)(η^3-2-Me-C_3H_4)}$_2$],[49] [{Pt(μ-Cl)(Naph^C*)}$_2$] (**A**),[33] [{Pt(μ-Cl)(CO_2Et-C^C*)}$_2$] (**B**),[35] [{Pt(μ-Cl)(NC-C^C*)}$_2$] (**C**) and **1C–4C**[36] were prepared following the literature procedures.

Synthesis of [PtCl(Naph^C*)(PPh_3)] (1A). PPh_3 (158.6 mg, 0.59 mmol) was added to a suspension of **A** (233.4 mg, 0.27 mmol) in dichloromethane (30 mL) at r.t. After 1 h of reaction, the solution was filtered through Celite and the solvent was removed under reduced pressure. The residue was treated with MeOH (5 mL), filtered, and washed with MeOH (2 mL) to give **1A** as a pale yellow solid. Yield: 282.2 mg, 76 %. Anal.Calcd for $C_{32}H_{26}ClN_2PPt\cdot CH_2Cl_2$: C, 50.49; H, 3.60; N, 3.57. Found: C, 50.82; H, 3.39; N, 3.50. ^{1}H NMR (400 MHz, methylene chloride-d_2): δ =7.75-7.83 (m, 6H, H_o (PPh_3)), 7.62 (d, $^3J_{12,11}$= 8.1, 1H, H_{12}), 7.53 (m, 1H, H_2), 7.34-7.46 (m, 10H, H_m (PPh_3), H_p (PPh_3) and H_{14}), 7.24 (ddd, $^3J_{11,12}$ = 8.1, $^3J_{11,10}$ = 7.0, $^4J_{11,9}$ = 1.3, 1H, H_{11}), 7.08 (m, $^3J_{H,Pt}$ = 68.6, 1H, H_7), 7.06 (ddd, $^3J_{10,9}$ = 8.1, $^3J_{10,11}$ = 7.0, $^4J_{10,12}$ = 1.2, 1H, H_{10}), 7.00 (m,1H, H_3), 6.62 (d, $^3J_{9,10}$= 8.1, 1H, H_9), 4.31 (s, 3H, H_4). ^{13}C{^{1}H} NMR plus HMBC and HSQC

(101 MHz, methylene chloride-d_2): δ = 171.9 (s, C_1), 146.1 (s, C_5), 138.5 (d, $^3J_{C7,P}$ =8.2, C_7), 135.9 (d, $^2J_{C,P}$ = 10.9, $^3J_{C,Pt}$ = 19.7, 6C, $C_o(PPh_3)$), 130.7 (s, 3C, $C_p(PPh_3)$), 128.3 (d,$^2J_{C,P}$ = 10.1, 6C, $C_m(PPh_3)$), 127.1, 127.0 (s, 2C, C_9 and C_{12}), 125.1, 125.0 (s, 2C, C_{11} and C_{10}), 124.7 (d, $^4J_{C,P}$ = 5.8, C_3), 114.7 (s, C_2), 107.5 (s, C_{14}), 38.5 (s, C_4). ^{31}P {^1H} NMR (162 MHz, methylene chloride-d_2): δ = 30.1 (s, $^1J_{P,Pt}$= 2913.5).^{195}Pt\{^1H\} NMR (85.6 MHz, methylene chloride-d_2): δ= –4210.5 (d). IR (ATR, cm^{-1}): ν = 303 (m, Pt-Cl). MS (MALDI+): m/z 664.3 $[Pt(Naph\text{^}C^*)(PPh_3)]^+$, 700.3 $[PtCl(Naph\text{^}C^*)(PPh_3)]^+$.

Synthesis of [PtCl(CO_2Et-C^C*)(PPh_3)] (1B). It was prepared following the method described for **1A**.PPh_3 (84.5 mg, 0.31mmol) and **B** (130.6 mg, 0.14 mmol). **1B** (Yield: 157.5 mg, 77%). Anal.Calcd for $C_{31}H_{28}ClN_2O_2PPt$: C, 51.56; H, 3.90; N, 3.88. Found: C, 51.95; H, 3.85; N, 3.89. ^1H NMR (400 MHz, methylene chloride-d_2): δ = 7.68-7.78 (m, 6H, H_o (PPh_3)), 7.61 (dd, $^3J_{9,10}$= 8.1,$^4J_{9,7}$ = 1.7, 1H, H_9), 7.55 (m, $^3J_{H,Pt}$ = 66.5, 1H, H_7), 7.33-7.46 (m, 10H, H_m (PPh_3), H_p (PPh_3) and H_2), 7.04 (d, $^3J_{10,9}$ = 8.1, $^4J_{H,Pt}$ = 22.1, 1H, H_{10}), 6.97 (m,1H, H_3), 4.30 (s, 3H, H_4), 3.94 (q, $^3J_{H,H}$ = 7.2, 2H, CH_2 (OEt)), 1.00 (t, $^3J_{H,H}$ = 7.2, 3H, CH_3 (OEt)). ^{13}C\{^1H\} NMR plus HMBC and HSQC (101 MHz, methylene chloride-d_2): δ = 172.0 (s, C_1), 166.3 (s, CO_2Et), 151.1 (s, C_5), 140.9 (d, $^3J_{C7,P}$ =9.5, C_7), 135.8 (d,$^2J_{C,P}$ = 11.2,$^3J_{C,Pt}$ = 22.0, 6C, $C_o(PPh_3)$), 131.4 (s, C_6), 130.9 (d, $^4J_{C,P}$ = 2.3, 3C, $C_p(PPh_3)$), 128.4 (d,$^2J_{C,P}$ = 10.5, 6C, $C_m(PPh_3)$), 125.9 (s, C_9), 124.5 (d, $^4J_{C,P}$ = 6.1, C_3), 114.5 (d, $^4J_{C,P}$ = 2.6, C_2), 111.0 (s, C_{10}), 60.6 (s, CH_2 (OEt)), 38.5 (s,C_4), 14.4 (s, CH_3 (OEt)). ^{31}P {^1H} NMR (162 MHz, methylene chloride-d_2): δ = 29.9 (s, $^1J_{P,Pt}$= 2910.9).^{195}Pt\{^1H\} NMR (85.6 MHz, methylene chloride-d_2):δ = –4247.0 (d). IR (ATR, cm^{-1}): ν = 286 (m, Pt-Cl), 1704 (m, C=O). MS (MALDI+): m/z 686.1 $[Pt(CO_2Et\text{-}C\text{^}C^*)(PPh_3)]^+$

Synthesis of [Pt(Naph^C*)(py)(PPh_3)]PF_6 (2A). Pyridine (16.0 μL, 0.20 mmol) and KPF_6 (37.5 mg, 0.20 mmol) were added to a pale yellow suspension of **1A** (139.6 mg, 0.20 mmol) in

acetone (30 mL). After 1 h of stirring at r.t., the solvent was evaporated to dryness and the residue treated with dichloromethane (35 mL) and filtered through Celite. Then, the solvent was removed under reduced pressure and the residue was treated with diethylether (10 mL), filtered and washed with diethylether (5 mL) to give **2A** as a pale yellow solid. Yield: 144.6 mg, 82%. Anal.Calcd for $C_{37}H_{31}F_6N_3P_2Pt$: C, 50.01; H, 3.52; N, 4.73. Found: C, 49.76; H, 3.28; N, 4.46. ^{1}H NMR (400 MHz, methylene chloride-d_2): δ =8.44 (d, $^3J_{H,H}$ = 6.6, $^3J_{H,Pt}$ = 21.7, 2H, H$_o$ (py)), 7.60-7.72 (m, 9H, H$_o$ (PPh$_3$), H$_p$ (py), H$_2$ and H$_{12}$), 7.51 (s, $^4J_{H,Pt}$ = 10.0, 1H, H$_{14}$), 7.45 (m, 3H, H$_p$ (PPh$_3$), 7.30-7.37 (m, 6H, H$_m$ (PPh$_3$)), 7.29 (ddd, $^3J_{11,12}$ = 8.1, $^3J_{11,10}$ = 7.0, $^4J_{11,9}$ = 1.2, 1H, H$_{11}$), 7.19 (m, 2H, H$_m$ (py)), 7.12 (ddd, $^3J_{10,9}$ = 8.1, $^3J_{10,11}$ = 7.0, $^4J_{10,12}$ = 1.2, 1H, H$_{10}$), 7.08 (d, $^3J_{7,P}$ = 2.4, $^3J_{H,Pt}$ = 61.2, 1H, H$_7$), 7.03 (m,1H, H$_3$), 6.82 (d, $^3J_{9,10}$= 8.1, 1H, H$_9$), 2.87 (s, 3H, H$_4$). ^{13}C{^{1}H} NMR plus HMBC and HSQC (101 MHz, methylene chloride-d_2): δ = 171.9 (d, $^2J_{C1,P}$ = 137.5, C$_1$), 152.4 (s, C$_o$ (py)), 146.1 (s, C$_5$), 141.1 (d, $^3J_{C7,P}$ =9.6, C$_7$), 139.5 (s, C$_p$ (py)), 135.2 (d, $^2J_{C,P}$ = 11.6, $^3J_{C,Pt}$ = 20.3, 6C, C$_o$(PPh$_3$)), 131.7 (s, 3C, C$_p$(PPh$_3$)), 129.1 (d,$^2J_{C,P}$ = 10.5, 6C, C$_m$(PPh$_3$)), 127.7 (s, C$_m$ (py)), 127.3, 127.1 (s, 2C, C$_9$ and C$_{12}$), 126.1 (s, C$_{11}$), 125.5 (s, C$_{10}$), 124.8 (d, $^4J_{C,P}$ = 5.0, C$_3$), 121.4 (s, C$_6$), 115.0 (s, C$_2$), 108.5 (s, $^4J_{C14,Pt}$ = 26.5, C$_{14}$), 35.6 (s, C$_4$). ^{31}P {^{1}H} NMR (162 MHz, methylene chloride-d_2): δ = 29.8 (s, $^1J_{P,Pt}$ = 2926.2).^{195}Pt{^{1}H} NMR (85.6 MHz, methylene chloride-d_2):δ= –4253.5 (d).IR (ATR, cm^{-1}): ν =829 (s, PF$_6$), 556 (s, PF$_6$). MS (MALDI+): m/z 664.3 [Pt(Naph^C*)(PPh$_3$)]$^+$. Λ_M (5x10^{-4} M acetone solution): 73.35 Ω^{-1} cm^{2}mol^{-1}.

Synthesis of [Pt(CO$_2$Et-C^C*)(py)(PPh$_3$)]PF$_6$ (2B). It was prepared following the method described for **2A.**Pyridine (24.7 µL, 0.31 mmol), KPF$_6$ (28.7 mg, 0.15 mmol) and **1B** (110.5 mg, 0.15 mmol). **2B** (Yield: 115.2 mg, 83 %). Anal.Calcd for $C_{36}H_{33}F_6N_3O_2P_2Pt$: C, 47.48; H, 3.65; N, 4.61. Found: C, 47.47; H, 3.65; N, 4.72. ^{1}H NMR (400 MHz, methylene chloride-d_2): δ = 8.45

(d, $^{3}J_{H,H}$ = 5.0, $^{3}J_{H,Pt}$ = 21.7, 2H, H_o (py)), 7.64-7.72 (m, 2H, H_p (py) and H_9), 7.56-7.64 (m, 6H, H_o (PPh_3)), 7.41-7.52 (m, 5H, H_2, H_7 and H_p (PPh_3)), 7.33 (m, 6H, H_m (PPh_3)), 7.21 (m, 2H, H_m (py)), 7.14 (d, $^{3}J_{10,9}$ = 8.2, $^{4}J_{H,Pt}$ = 11.0, 1H, H_{10}), 7.07 (m,1H, H_3), 3.92 (q, $^{3}J_{H,H}$ = 7.1, 2H, CH_2 (OEt)), 2.90 (s, 3H, H_4), 0.95 (t, $^{3}J_{H,H}$ = 7.1, 3H, CH_3 (OEt)). $^{13}C\{^{1}H\}$ NMR plus HMBC and HSQC (101 MHz, methylene chloride-d_2):δ = 172.8 (d, $^{2}J_{C1,P}$ = 136.2, C_1), 165.9 (s, CO_2Et), 152.4 (s, C_o (py)), 151.3 (s, C_5), 142.4 (d, $^{3}J_{C7,P}$ = 9.7, C_7), 139.8 (s, C_p (py)), 135.2 (d, $^{2}J_{C,P}$ = 11.5,$^{3}J_{C,Pt}$ = 21.1, 6C, C_o(PPh_3)), 132.0 (d, $^{4}J_{C,P}$ = 2.0, 3C, C_p(PPh_3)), 129.3 (d, $^{3}J_{C,P}$ = 10.8, 6C, C_m(PPh_3)), 128.0 (s, C_m (py)), 127.8 (s, C_9), 124.9 (d, $^{4}J_{C,P}$ = 4.8, C_3), 122.9 (d, $^{2}J_{C,P}$ = 6.2, C_6), 115.5 (d, $^{4}J_{C,P}$ = 2.3, C_2), 111.6 (s, $^{3}J_{C,Pt}$ = 29.2, C_{10}), 60.7 (s, CH_2 (OEt)), 35.9 (s, C_4), 14.3 (s, CH_3 (OEt)). $^{31}P\ \{^{1}H\}$ NMR (162 MHz, methylene chloride-d_2): δ = 29.2 (s, $^{1}J_{P,Pt}$= 2930.0). $^{195}Pt\ \{^{1}H\}$ NMR (85.6 MHz, methylene chloride-d_2): δ = –4288.0(d). IR (ATR, cm^{-1}): ν =832 (s, PF_6), 556 (s, PF_6), 1707 (m, C=O). MS (MALDI+): m/z 686.1 $[Pt(CO_2Et\text{-}C\text{^}C^*)(PPh_3)]^+$. Λ_M ($5x10^{-4}$ M acetone solution): 71.84 Ω^{-1} cm^2 mol^{-1}

RESULTS AND DISCUSSION

Synthesis and characterization of [PtCl(R-C^C*)(PPh_3)] and [Pt(R-C^C*)(py)(PPh_3)]PF_6

The dinuclear complexes [{Pt(μ-Cl)(R-C^C*)}$_2$] (R-C = Naph (**A**), R = CO_2Et (**B**)) react with PPh_3 in a 1:2 molar ratio in dichloromethane at room temperature (Scheme 1, path a and Experimental Section) to give the mononuclear complexes *trans*-(C*, P) [PtCl(R-C^C*)(PPh_3)] (R-C = Naph **1A**, R = CO_2Et **1B**). Then, compounds [Pt(R-C^C*)(py)(PPh_3)]PF_6 (R-C= Naph **2A**, R= CO_2Et **2B**) were synthesized by treating **1A** and **1B** with one equivalent of KPF_6 and excess of pyridine in acetone at room temperature (see Scheme 1, path b and Experimental Section); they were isolated from their solutions as pure solids in high yields (ca. 83 %).

All the spectroscopic and crystallographic data discussed below support the formulation proposed for all of these new compounds and their *trans*-(C*, PPh_3) geometry, like in the previously reported compounds **1C**-**4C**.[36]

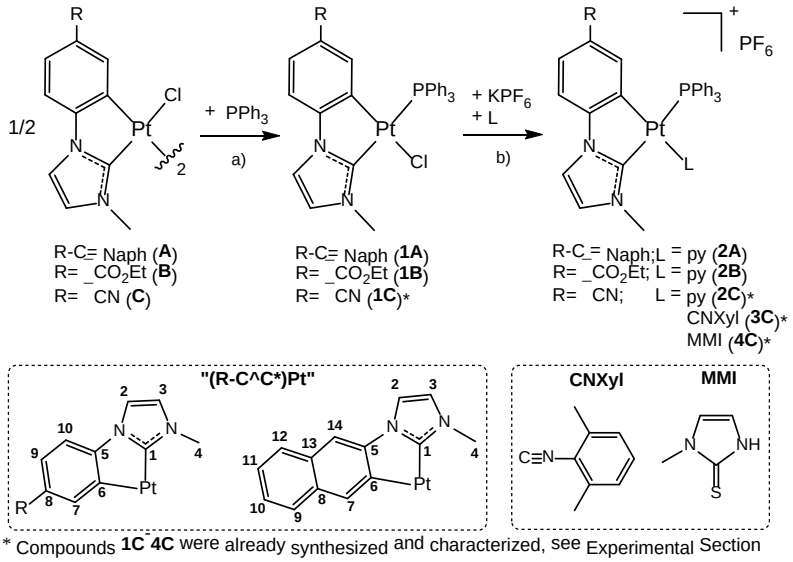

* Compounds **1C**-**4C** were already synthesized and characterized, see Experimental Section

Scheme 1. Syntheses of compounds

Very relevant structural information was provided by multinuclear NMR spectra. The ^{1}H NMR spectra of **1A**, **1B**, **2A** and **2B** show the expected signals for the C^C* group and the auxiliary ligands with intensity ratios corresponding to the proposed stoichiometries (see Experimental Section and the SI, Figures S1-S4). It is worth noting that resonances corresponding to H7, H9 and H10 protons in compounds **1A** and **2A** appear more shielded than the H14, H12 and H11 ones due to the anisotropic effect caused by the proximity in space of the aromatic ring current of the phenyl group of the PPh_3. This same phenomenon is also observed in the H4 resonance of complexes **2A** and **2B** (δ~ 2.90 ppm) which undergoes an important upfield shift when compared with those of the corresponding chloride counterparts, **1A** and **1B**, (δ~ 4.30 ppm). In this case, the anisotropic shielding effect is associated to the pyridine ring coordinated in a *cis* position to

the carbenic fragment.[36] In agreement with their formulation, the $^{31}P\{^{1}H\}$ NMR spectra of **1A**–**2B** show only one sharp signal at *ca*. 30 ppm flanked by platinum satellites, and their $^{195}Pt\{^{1}H\}$ NMR spectra exhibit the expected doublets ranging from –4210.5 to –4288.0 ppm (see Experimental Section and Figure S5). The δP, δPt and $^{195}Pt–^{31}P$ coupling constants are very similar to those found in the related complexes **1C** and **2C**,[36] with a *trans*-(C*, PPh_3) geometry, and are in the range of complexes with a P−Pt−C *trans* arrangement,[50-52] making evident the strong *trans* influence of the carbene atom (C*) of the two R-C^C* groups (R-C = Naph, R = CO_2Et) as well. As inferred from the ^{195}Pt NMR spectral data, the naphthyl derivatives (**1A** and **2A**) appear downfield shifted (17 - 37 ppm) with respect to those of the ethoxycarbonyl (**1B** and **2B**) and the cyano ones (**1C** and **2C**), indicating that the larger π system induces an important withdraw of electron density from the platinum center. These spectral and electronic features were also observed in related compounds $[Pt(R\text{-}C\hat{}C^*)(CNR')_2]PF_6$.[35] In addition, the $^{13}C\{^{1}H\}$ NMR spectra of **2A** and **2B** revealed the presence of a doublet at ~172 ppm with a $^{31}P\text{-}^{13}C$ coupling constant value of *ca*. 136 Hz, corresponding to the quaternary carbenic carbon (C1). However those of **1A** and **1B** could be only detected by 2D $^{1}H\text{-}^{13}C$ HMBC correlation experiments (see SI, Figures S1 and S2).

As inferred from these NMR data the cleavage of the bridging system rendered compounds *trans*-(C*, PPh_3)-[PtCl(R-C^C*)(PPh_3)] (R-C = Naph **1A**, R = CO_2Et **1B**) as a unique isomer and the subsequent replacement of Cl by py in the coordination environment of Pt proceeds with stereoretention giving compounds *trans*-(C*, PPh_3)-[Pt(R-C^C*)(py)(PPh_3)]PF_6 (R-C= Naph **2A**, R= CO_2Et **2B**). These results were the expected ones considering the degree of transphobia (T) of pairs of ligands in *trans* positions.[53-57] In our previous work we concluded that $T[C_{Ar}/L)] > T[C^*/L]$ and $T[C_{Ar}/PPh_3)] > T[C_{Ar}/py)] > T[C_{Ar}/Cl)]$, in such a way that the $T[C_{Ar}/PPh_3)]$ should

be the greatest one. The current experimental results indicated that, as it was observed in case of compounds **1C–4C**, the difference between T[C_{Ar}/PPh_3)] and T[C*/PPh_3] is big enough to direct the selective formation of *trans*-(C*, PPh_3)-complexes **1A–B**, **2A–B** as pure compounds. This conclusion was confirmed by the single crystal X-ray diffraction analysis of **2A** and **2B** shown in the following.

Crystal Structure Determination of [Pt(R-C^C*)(py)(PPh_3)]PF_6

The crystal structures of **2A** and **2B** have been determined by X-ray diffraction studies (Figures1 and S6-S8, Table S1). The asymmetric unit of **2A** contains two molecules (Pt1 and Pt2) with similar structural details (see Figure S6). The platinum(II) center exhibits a distorted square-planar environment due to the small bite angle of the NHC cyclometalated ligands (R-C^C*) [79.48(13) –80.09(13)º]. This C–Pt–C bite angle and both Pt–C bond lengths are similar to those observed for other five-membered metalacycles of Pt(II) with N-heterocyclic carbenes.[26-30, 33, 35, 36, 58-60] PPh_3 and pyridine complete the coordination sphere of the platinum center. The Pt–N,[36, 61-64] and Pt–P[36, 50, 65-68] bond distances are within the typical range for platinum (II) compounds with these *trans* to σ-bonded carbon atoms. The pyridine rings are placed almost perpendicular to the platinum coordination planes (Pt, C, C, P, N) with dihedral angles of 85.44° (Pt1, **2A**), 80.20° (Pt2, **2A**) and 74.89° (**2B**). In their crystal structure packings, intra- and very weak inter-molecular interactions were observed (Figures S7, S8). As observed in the ^{1}H NMR spectra, there are C–H···π intramolecular interactions between the Me groups (C4/C41) and the pyridine rings in **2A** [d(C4···C_g = 3.267 Å) and d(C41···C_{g2} = 3.381 Å)] whereas in **2B** those contacts are significantly longer [d(C4···C_g = 3.788 Å); C_g are the centroids of the pyridine rings]. Also, there are π···π intramolecular interactions (3.11 – 3.59 Å) between one of the phenyl groups of the PPh_3 and the pyridine rings.

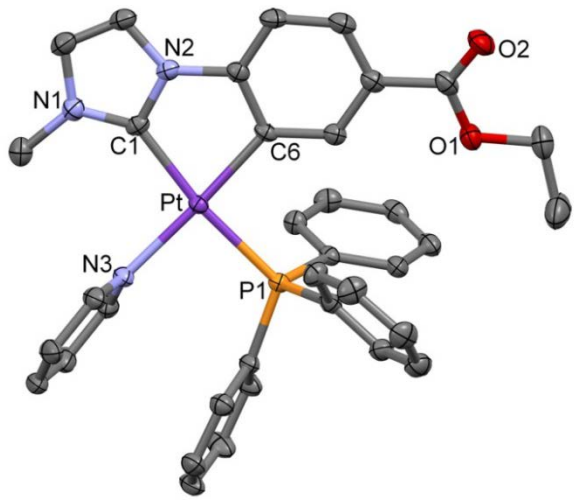

Figure 1. Molecular structure of the complex cation of **2B**. Selected bond lengths (Å) and angles (deg): Pt-C(1) 2.031(3); Pt-C(6) 2.035(3); Pt-P(1) 2.3031(8); Pt-N(3) 2.116(3); C(1)-Pt-C(6) 79.48(13); C(6)-Pt-P(1) 93.08(9); C(1)-Pt-N(3) 96.81(12); P(1)-Pt-N(3) 90.94(8). Solvent molecules, PF_6^- and hydrogen atoms have been omitted for clarity. Thermal ellipsoids are drawn at the 50% probability level.

In **2A**, the molecules arrange themselves in head-to-tail pairs, showing a clear offset stacking with rather long intermolecular π···π contacts (~ 3.50 Å, see Figure S7) whereas in **2B** the molecules are located far apart with no π···π interactions between each other.

Additionally, in both crystal structures (**2A** and **2B**) there are some weak C-H···F contacts (d C–F= 3.03 Å; d H–F= 2.30 Å, see Figure S8)[69-71] between the cationic complexes and the PF_6^- anion which is in agreement with the low conductivity measurements.

Photophysical properties of compounds [Pt(R-C^C*)(py)(PPh_3)]PF_6 (R-C = Naph (2A); R = CO_2Et (2B), CN (2C)) and [Pt(NC-C^C*)(PPh_3)L]PF_6 (L = CNXyl (3C), MMI (4C)).

In this section we compare the absorption and emission properties of two sets of compounds, **2A**–**2C** and **2C**–**4C,** aiming to study how the photophysical properties of these ionic compounds

are affected by the variation of the NHC group or the ancillary ligands respectively. UV–vis spectra data of **2A**–**4C** are listed in Table S2. As shown in Figure 2, in diluted CH_2Cl_2 solution they all display strong absorption bands at $\lambda \leq 300$ nm ($\varepsilon > 10^4$ $M^{-1}cm^{-1}$) which are normally attributed to the ^{1}IL transitions of the NHC ligand.

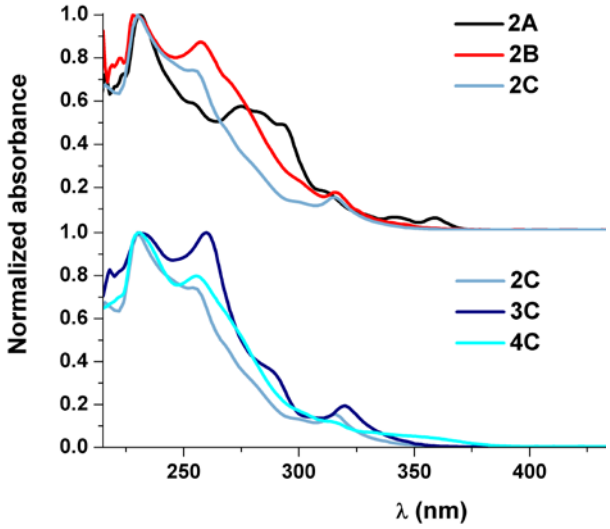

Figure 2. Normalized absorption spectra in CH_2Cl_2 ($5x10^{-5}$ M) at r.t.

Complexes **2B** and **2C** show almost identical UV-vis spectra with the lowest-energy absorption at around 315 nm ($\varepsilon \sim 10^3$ $M^{-1}cm^{-1}$), suggesting that the electronic features of the R-C^C* (R = CO_2Et, CN) ligands are comparable and quite different from those of the naphthyl counterpart, **2A**.

The latter exhibits an additional low energy band at $\lambda \sim$ 350 nm ($\varepsilon \sim 10^3$ $M^{-1}cm^{-1}$) which is very similar to that observed in complexes with the same cyclometalated NHC ligand (Naph^C*).[33, 35] It appears slightly shifted to higher energies when compared to the isocyanide derivatives, $[(Naph^C*)Pt(CNR')_2]PF_6$ (R' = *t*-Bu, Xyl),[35] which indicates the participation of the ancillary ligands in it. The involvement of the auxiliary ligands in the lowest energy absorptions can also be noticed for complexes **2C**–**4C**. The one corresponding to the isocyanide derivative, **3C** (λ=

320 nm), is shown clearly red-shifted with respect to the pyridine one, **2C** (λ= 316 nm). While that of **4C**, becomes a less intense shoulder (λ= 314 nm) accompanied with an additional band at λ= 352 nm. This lowest-energy absorption of **4C** (352 nm) obeys Beer's Law, suggesting that it is due to transitions in the molecular species and that no significant aggregation occurs within the concentration range from 10^{-3} to 10^{-6} M (see Figure S9). UV-Vis spectra of all complexes were recorded in different solvents (Table S2) showing no significant solvatochromism, except for compound **2A** (see Figure S10). It presents a slight negative solvatochromism in the lower energy spectral region (λ> 340 nm), which indicates the existence of charge transfer (CT) transitions.[72]

Solid state diffuse reflectance spectra are depicted in Figure S11. They show no particular differences when compared to those observed in solution of CH_2Cl_2. Therefore, the weak intermolecular π-π and C-H···F interactions observed in their X-ray structures (at *ca* 100 K) seem to have no important effects in the absorption at room temperature.

DFT and TD-DFT calculations in solution of CH_2Cl_2 for **2A–2C** and **4C** have been carried out to provide correct assignments for the UV-vis absorptions and also, to evaluate the effect of both, cyclometalated R–C^C* and ancillary ligands (L) on the photophysical properties.

The optimized geometries of the ground state, S_0, and T_1 (Tables S3-S10) were carried out at the M06/SDD(Pt)/6-31G*(ligands atoms) level. The geometric parameters of the optimized structures (S_0) agree reasonably well with the experimental values (Tables S11 and S12). Diagrams of the frontier molecular orbitals (FOs) in the ground state are depicted in Figure S12 and the relative compositions of the different energy levels are reported in Table 1. Excitation energies at the ground state geometry were calculated by TD-DFT in CH_2Cl_2 solution and selected low-lying transitions are listed in Table S13. The composition of the FOs of **2B** and **2C**

are practically identical, which confirm the similarities of the electronic features of the R-C^C* (R = CN, CO_2Et) cyclometalated groups. In these cases the HOMOs are mainly constructed from π-orbitals of the C^C* ligand (ca. 75%) and dπ-orbitals of the Pt center (25 %) and the LUMOs are similar to the HOMOs but with some contribution of the ancillary ligands: 20% Pt, ca. 65% C^C*, 8% PPh_3 and 7% py. However, in case of **2A**, the HOMO is almost entirely localized on the Naph^C* fragment (90%) while the LUMO is mostly centered on the pyridine (70%) with a little contribution of Naph^C*(ca. 15%) and Pt orbitals (ca. 10%). By comparing **2C** and **4C**, it can be observed that in **4C** the presence of MMI instead of py in the coordinating sphere of platinum leads to a HOMO mainly based on the auxiliary ligand (MMI, 85%) with only a low contribution of Pt and R-C^C*orbitals, while no significant changes are induced in the LUMO composition with respect to that in **2C**, which is mostly centered on the R-C^C* orbitals. Thus, by modifying both ligands, either the R-C (C^C*) or L, the nature and composition of the FOs change considerably and therefore, the nature of the lowest energy singlet transition. The calculated S_1 in CH_2Cl_2 arises from HOMO to LUMO transition for **2B**, **2C** and **4C** while for **2A** arises mainly from H→L (39%) and H→L+1 (36%) transitions.

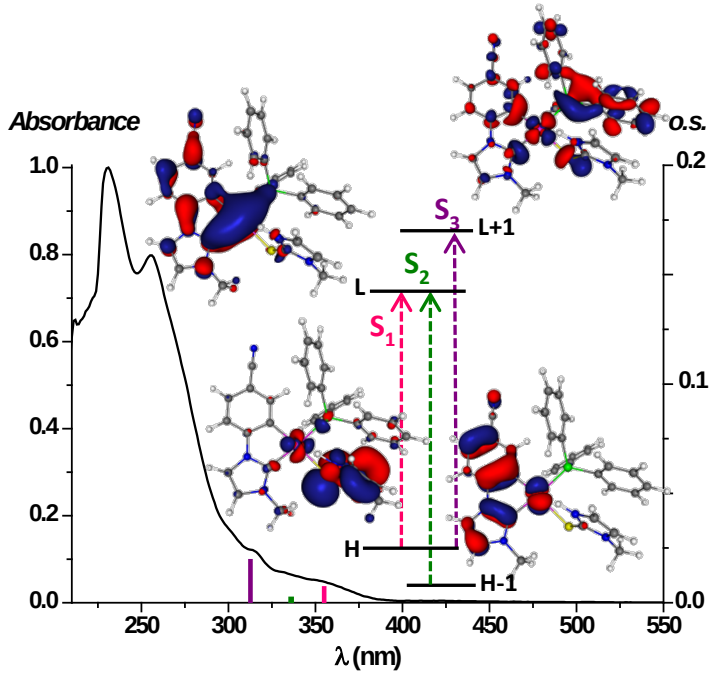

Figure 3. Normalized UV−vis absorption spectrum of **4C** in CH_2Cl_2, calculated transitions in CH_2Cl_2 (colored bars) with the diagrams of the frontier orbitals.

Considering that the calculated allowed absorptions are in good qualitative agreement with the experimental UV-vis spectra (Figures 3, S13–S15) the lowest energy absorption bands can be attributed to mixed transitions: ILCT [(NHC)]/LL'CT [π(NHC) →π*(L')] for **2B** and **2C** and LL'CT [π(NHC) →π*(py)]/ ILCT [π(NHC) →π*(NHC)]/LMCT [π(NHC) → 5d(Pt)] for **2A** and L'LCT [π*(MMI) →π*(NHC)]/L'MCT [π*(MMI) → 5d(Pt)] for **4C**. Complex **4C** shows also a very weak calculated absorption at 336 nm (S_2, see Figure 3) that implicates the H–1→L (95%) transition. Its energy and electronic nature are very similar to the calculated S_1 transition in complexes **2B** and **2C**.

Table 1. Population analysis (%) of frontier MOs in the ground state for 2A–2C and 4C in solution of CH_2Cl_2

MO	eV				Pt				R-C^C*				PPh_3				L			
	2A	2B	2C	4C	2A	2B	2C	4C	2A	2B	2C	4C	2A	2B	2C	4C	2A	2B	2C	4C
L+1	-1.57	-1.66	-1.72	-1.37	26	5	5	23	34	7	4	25	14	1	1	46	26	87	90	6
L	-1.72	-1.89	-1.99	-2.00	11	20	20	23	15	64	69	67	4	8	7	7	70	8	4	3
H	-6.28	-6.72	-6.88	-6.46	9	25	24	9	90	74	75	3	1	1	1	3	0	0	0	85
H-1	-6.60	-7.16	-7.24	-6.85	18	61	56	24	80	8	4	74	1	30	39	1	1	1	1	1

Emission data are summarized in Table 2. The phosphorescence of all complexes in CH_2Cl_2 (10^{-5} M, 298 K) is quenched, even under Ar atmosphere, which may be due to thermal non radiative processes.[34] Nonetheless, in a rigid matrix (CH_2Cl_2 solution at 77 K), these molecules show bright and long live luminescence. All compounds show well resolved vibronic emissions and their excitation profiles mimic the corresponding UV-Vis absorptions. In case of **2A,** containing Naph^C* cyclometalated group, the phosphorescence appears at λ_{max}~ 474 nm with a monoexponential decay substantially long (~ 480 μs). The analogous complexes, **2B**, **2C**, as well as **3C** and **4C**, all of them containing the R-C^C* (R = CN, CO_2Et) cyclometalated groups, exhibit a phosphorescent emission (λ_{max}~ 450 nm) blue-shifted with respect to **2A** (see Figure 4) and shorter decays (about 20 μs). Among those complexes containing the NC-C^C* cyclometalated group, **2C–4C**, the Xyl derivative (**3C**) produces an emission slightly shifted to lower energies with respect to **2C** and **4C**. The emissive behavior (emission energy and lifetime) of **2A** in CH_2Cl_2 rigid matrix is very similar to that observed in other compounds containing the same "(Naph^C*)Pt" fragment.[33, 35] Thus, taking into account all these data and the TD-DFT calculations, the phosphorescent emissions of **2A** can be mainly assigned to ^{3}ILCT [(NHC)] transitions mixed with some, if any, ^{3}LL'CT [π(NHC) $\rightarrow\pi^*$(L)]/^{3}LMCT [π(NHC) $\rightarrow$ 5d(Pt)] character. The emission bands of **2B** and **2C–4C** are tentatively ascribed to transitions of monomeric species derived from ^{3}ILCT [(NHC)]/^{3}LL'CT [π(NHC) $\rightarrow\pi^*$(L')] excited states. It is worth noting that the low energy absorption (S_1) of **4C** was attributed in the UV-Vis Section to mixed transitions L'LCT [π^*(MMI) $\rightarrow\pi^*$(NHC)]/L'MCT [π^*(MMI) $\rightarrow$ 5d(Pt)]. However, the emission features are identical to those observed for **2B**, **2C** and **3C**, which correspond to the assignment of the S_2 calculated absorption.

Table 2. Photophysical data for complexes 2A–2C, 3C and 4C.

Com.	Media (T/K)	λ_{ex} (nm)	λ_{em} (nm)	τ (μs)[d]	ϕ[e]
2A	CH_2Cl_2[a](77)	355	474_{max}, 511, 551, 598	481	
	CH_2Cl_2[b] (77)	357	474_{max}, 511, 551, 598	478	
	PMMA Film	340	476_{max}, 511, 600_{sh}		0.87
	Solid (298)	368	557, 600_{max}, 650	35	0.06
	Solid (77)	361	541_{sh}, 552, 581_{sh}, 597_{max}, 648_{sh}	65	
2B	CH_2Cl_2[a](77)	315	444_{max}, 475, 506, 545_{sh}	23	
	CH_2Cl_2[b] (77)	360	447_{max}, 477, 509, 545_{sh}	24	
	PMMA Film	330	448, 476_{max}, 503, 543_{sh}		0.68
	Solid (298)	360	455, 474_{max}, 501	2.6	0.19
	Solid (77)	364	455, 474_{max}, 505	15	
2C	CH_2Cl_2[a](77)	314	444_{max}, 474, 505, 538_{sh}	23	
	CH_2Cl_2[b] (77)	355	447_{max}, 477, 509, 538_{sh}	22	
	PMMA Film	320	446, 472_{max}, 500, 540_{sh}		0.93
	Solid (298)	350	446, 472_{max}, 500, 540_{sh}	17	0.35
	Solid (77)	355	447, 469_{max}, 500, 540_{sh}	25	
3C	CH_2Cl_2[a](77)	320	449_{max}, 480, 513, 543	26.9	
	CH_2Cl_2[b] (77)	350	450, 483_{max}, 515, 545, 615	24	
		400	545_{max}, 615_{sh}	1.6	
		450	545_{sh}, 615_{max}	2.0	
	PMMA Film	340	453, 480_{max}, 511, 550_{sh}		0.87
	Solid (298)	465	590	1.2	0.11
	Solid (77)	350	465, 488_{max}, 524	20	
		390	465, 488, 545_{max}	1.8	
		460	545_{sh}, 615_{max}	2.2	
4C[c]	CH_2Cl_2[a](77)	314, 355	444_{max}, 474, 506, 543_{sh}	19	
	CH_2Cl_2[b] (77)	320, 375	449_{max}, 479, 512, 548_{sh}	14	
		450	558	4	
	Solid (298)	370	449, 474_{max}, 505, 538_{sh}	2.6	0.11
	Solid (77)	370	444, 474_{max}, 506, 538_{sh}	12.7	

a = 10^{-5}M; *b* = 10^{-3}M; *c* = not soluble to prepare PMMA films in CH_2Cl_2 10^{-2} M; *d*= measurements at λ_{max}; *e* = PMMA films in Ar atmosphere.

In fact, if assuming the lowest energy absorption (S_1) as the emissive state, the geometry of the first excited state (T_1) should show a decrease of the Pt-S bond distance with respect to that of the ground state (S_0) (see Table S11) since an electron would be promoted from a dπ*(Pt/S(MMI)) antibonding orbital in the excitation process (see HOMO in Figure 3 or S12).

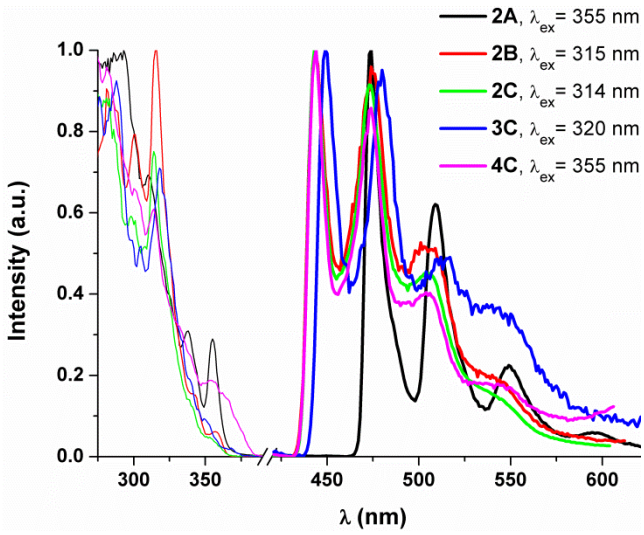

Figure 4. Normalized excitation (—) and emission (**▬**) spectra in rigid matrix of CH_2Cl_2 (10^{-5} M) at 77 K.

But this is not observed and the Pt-S distance remains invariable (Δ= 0.01). Nonetheless, there is a shortening of the Pt-C6 and Pt-C1 distances in the T_1 structure when compared to those of the S_0 one, which may be attributed to promoting an electron from a dπ*(Pt/NHC) antibonding orbital (see HOMO-1 in Figure 3 or S12) in the excitation process. This same shortening is also detected in the T_1 structures of **2B** and **2C**. Thus, the emissive behavior of **2B**, **2C** and **4C** is practically identical and seems to arise from the S_1 (**2B** and **2C**) and S_2 (**4C**) low lying absorptions. At higher concentration (10^{-3} M), the pyridine-complexes **2A**–**2C** display the same emission profiles and lifetimes than those obtained in diluted solution (10^{-5} M) whereas for **3C** and **4C**, the emission profile depends on the excitation wavelength. In complex **3C**, when monitoring the spectra at λex = 400 nm, an unstructured low energy (LE) band at 545 nm becomes the predominant while one emission at 615 nm can be selectively tuned by exciting at λex = 450 nm. In complex **4C**, a LE emission band at 558 nm is observed upon excitation at 450 nm (see Figure S16). The excitation maxima of these LE bands appearing the low energy

spectral region (~ 400 and 450 nm), and their lifetime decays (in the order of 2–4 μs) are shorter than those of the monomer emissions. As a result of taking all this into consideration, we tentatively ascribe these LE bands to $^3\pi\pi^*$ transitions from aggregates formed by intermolecular interactions. This wavelength dependent behavior was formerly observed in some of the isocyanide derivatives $[Pt(C\hat{}C^*)(CNR)_2]PF_6$.[35]

The spectra of poly(methyl methacrylate) (PMMA) films of all of these complexes perfectly match with those in rigid matrix of CH_2Cl_2 (see Figure 5 and Table 2). Thus, the origin of the emissions for all complexes in PMMA seems to be the same as those in rigid matrix. Quantum yield (QY) measurements revealed that all complexes are very good blue-emitters at room temperature. To the best of our knowledge, the QY values (68% – 93%) are amongst the highest ones for blue emitters of platinum(II).[25, 26, 28-30, 32, 34, 58, 73]

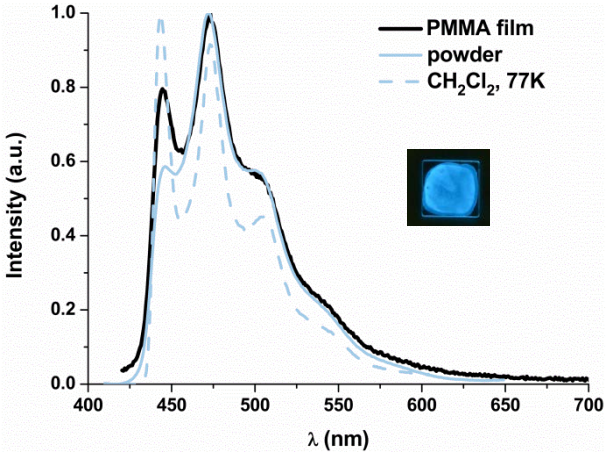

Figure 5. Normalized emission spectra of **2C**. Picture taken under UV light (λ_{ex} = 365 nm).

Experiments with pure powders showed that at 298 K and 77 K, complexes **2B**, **2C** and **4C** exhibit a phosphorescent blue emission (see Figure 6) with patterns and lifetimes very similar to those in rigid matrix of CH_2Cl_2.

Hence, their emissions are most likely originated from the same excited states. However, the naphthyl derivative, **2A**, shows an orange emission with maximum at *ca*. 600 nm either at 298 K or at 77 K (see Figures 6 and S17) instead of the blue one displayed in PMMA and rigid matrix of CH_2Cl_2. Its apparent vibronic spacings [1286 cm^{-1}], that match the skeletal vibrational frequency of the NHC ligand, and the lifetime values allow it to be ascribed to $^3\pi\pi^*$ transitions from aggregates formed by intermolecular $\pi\cdots\pi$ interactions among the "Naph^C*" moieties.[25, 33, 35]

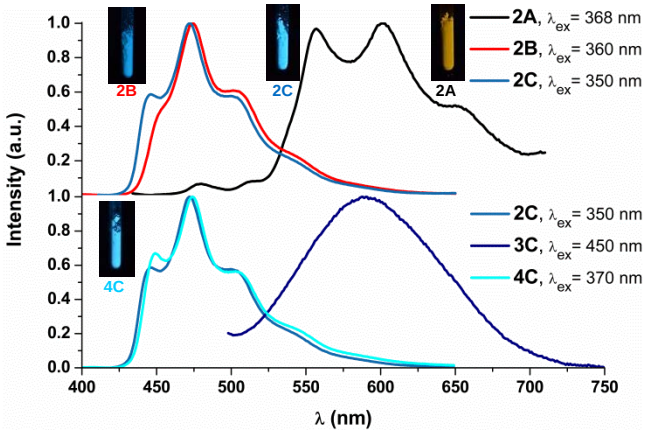

Figure 6. Normalized emission spectra in solid state at 298 K. Pictures under UV light (λ_{ex} = 365 nm).

Complex **3C** shows at 298 K an unstructured broad band with maximum at 590 nm that fit to a short monoexponential decay (τ= 1.2μs). Upon cooling to 77 K, the emissive behavior resembles to the wavelength dependent one registered in rigid matrix of CH_2Cl_2 (10^{-3} M) (see Figure S18). Quantum yield (Φ) measurements carried out on neat solid powders (35% – 6%) revealed that the emissions are generally quenched because of the presence of dioxygen in the measuring chamber. The QY value results particularly low for complex **2A**, which could be attributed to the low efficiency of the emissive $^3\pi\pi^*$ excited states.

The thermo-gravimetric analysis (TGA) of these blue-emitters indicated that under argon at 1 atm. they are stable at temperatures over 200°C [247.31ºC **2A**, 244.47ºC **2B**, 206.82ºC **2C**, 269.64ºC **3C**, 239.12ºC **4C**].

Electroluminescence

2C and **3C** were chosen to fabricate OLEDs with blue and yellow-orange emission, respectively, while devices containing mixtures of the two have been considered in order to obtain intermediate colors (i.e. white light emission). Despite the conventional approach used for solution processable organometallic Pt complex is their dispersion into a conjugated host matrix with proper additives to achieve good charge carrier balancing, we explore here a simpler bilayer structure consisting in a hole injection layer covered with the neat compound as EML, thanks to its good film forming ability. As hole injection layer a film of polyvinylcarbazole (PVK) is deposited onto the ITO/PEDOT:PSS coated glass by following the procedure reported elsewhere.[74] Afterwards a neat film of **2C** or **3C** is deposited by spincoating from a $CHCl_3$ solution. This simple and unconventional, for organometallic phosphors, device architecture exhibited unexpected good electro-optical performances.

In Figure 7 the electroluminescence (EL) spectra of **2C**, **3C** and of four mixtures of them at different weight ratios are reported. The EL spectrum of **2C** well corresponds to its photoluminescence (PL) spectrum with a structured blue emission at 452 and 478 nm (see Figure S19). The EL spectrum of **3C** displays the broad band at 550 nm associated to its excimer emission (see Figure S20). The EL spectra of the **2C**:**3C** mixtures with a **3C** content of 50% or higher display mainly the emission of **3C** while a balanced emission from the two compounds is obtained for the device with a **3C** content of 10-20%, giving nearly white light emission (see Figures 7 and S21). The situation is quite different in the corresponding PL spectra, whose

dominant emission comes from the **2C** compound (see Figure S22). The different behaviors of the PL and EL spectra of the **2C**:**3C** mixtures is mainly related to the higher efficiency of the **3C** based device, when compared to the **2C** one (see Table 3). These observations suggest a more favorable energy barrier for carrier injection in **3C**, in agreement with the positions of their HOMO-LUMO energy levels (see Figure S23). Despite the devices are not optimized in terms of Pt-complex layer thickness and charge carrier regulation, they display encouraging good performance (see Table 3 and Figure S24) and stability, if considering the simple and unusual bilayer devices architecture unexplored for organometallic complexes processed by solution methods.

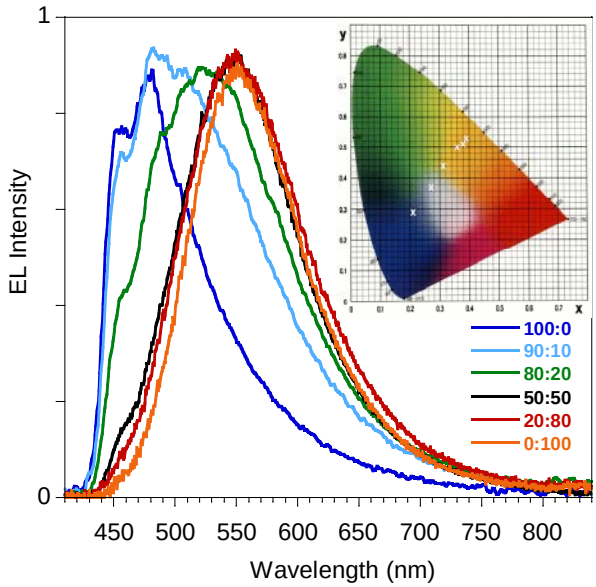

Figure 7. EL spectra of ITO/PEDOT:PSS/PVK/EML/Ba/Al devices with EML of spin-coated **2C**, **3C** and **2C**:**3C** at different weight ratios, driven at 5 V. The CIE 1931 chromaticity diagram is reported with the (x, y) position of the OLEDs emissions.

Table 3. OLEDs performances

weight ratio		EQE (%)	L_{MAX} (cd/m^2)	CIE 1931
2C	**3C**			**(x, y)**
0	100	0.3	50	(0.39;0.53)
20	80	0.2	101	(0.38:0.51)
50	50	0.1	9	(0.36;0.50)
80	20	0.02	5	(0.31;0.44)
90	10	0.007	6	(0.27;0.37)
100	0	0.01	4	(0.21;0.29)

CONCLUSIONS

In this work, we report the selective synthesis of new heteroleptic NHC cycloplatinated compounds [PtCl(R-C^C*)(PPh_3)] (R-C = Naph **1A**, R = CO_2Et **1B**) and [Pt(R-C^C*)(py)(PPh_3)]PF_6 (R-C = Naph **2A**, R = CO_2Et **2B**) as a sole isomer, the *trans*-(C*, PPh_3) one. As previously observed in the synthesis of compounds [PtCl(NC-C^C*)(PPh_3)] **1C** and [Pt(NC-C^C*)(PPh_3)L]PF_6 (L= py **2C**, CNXyl **3C**, MMI **4C**), the difference between T[CAr/PPh_3)] and T[C*/PPh_3] resulted to be large enough to direct the clean formation of the *trans*-(C*, PPh_3) isomer, in such a way that this feature seems to be of general application.

Compounds **2A–2C**, **3C** and **4C** prove to be among the most efficient Pt(II) blue- or greenish-blue emitters in PMMA films with QY values, measured under Ar atmosphere, ranging from 68% **2B** to 93% **2C**. The emission properties of all of them match with those in rigid matrix of CH_2Cl_2. In these conditions, no significant changes in the emission properties of compounds **2C–4C**, differing only in the nature of one ancillary ligand, were observed. Comparison of the

emission properties of compounds **2A–2C** differing only in the R-C^C* group, shows that in **2A** the larger π system induces an important withdraw of electron density from the platinum center, resulting in a bathochromic shift of its emission (ca. 30 nm) with respect to those of the analogous **2B** and **2C,** and in a much slower emissive decay because of the predominant ILCT character of its emission. Both experimental data and TD-DFT calculations bring to light the practically identical electronic features of the R-C^C* moiety (R = CN, CO_2Et). In the solid state, as much **2A** as **3C** show a weak yellowish-orange emission attributable to π-π* excited states of aggregates formed by intermolecular π···π interactions. Compounds **2C** and **3C** were chosen to fabricate OLEDs. Thanks to the good processability of the compounds, this is the first example of Pt-based devices fabricated by a full solution process technology with a non-doped emitting layer (EML). This very simple approach allowed us to tune the OLEDs emission from blue (**2C**) to yellow-orange (**3C**), passing through white (mixtures of **2C**:**3C**).

ASSOCIATED CONTENT

Supporting Information

The Supporting Information is available free of charge on the ACS Publications website.

General procedures and instrumentation, crystallographic and computational details; ^{1}H, $^{13}C\{^{1}H\}$, $^{195}Pt\{^{1}H\}$ NMR spectra of **1A**, **1B**, **2A** and **2B** spectra; X-ray crystallographic data and structures; UV-Vis data and figures; DFT and TD-DFT calculations; emission spectra, cyclic voltammograms and electroluminescence spectra (PDF); Crystallographic data for compounds **2A** and **2B** (CIF)

AUTHOR INFORMATION

Corresponding Author

*E-mail: sicilia@unizar.es

ACKNOWLEDGMENT

This work was supported by the Spanish Ministerio de Economía y Competitividad (MINECO)/FEDER (Project CTQ2015-67461-P led by Dr. Babil Menjón) and the Departamento de Industria e Innovación del Gobierno de Aragón and Fondo Social Europeo (Grupo Consolidado E21: Química Inorgánica y de los Compuestos Organometálicos led by Dr. José M. Casas). The authors thank the Centro de Supercomputación de Galicia (CESGA) for generous allocation of computational resources.A. C. acknowledges the support of a FPI grant from the Spanish government. U.G. and C.B. acknowledge the support of Project I-Zeb, III Accordo Quadro CNR -Regione Lombardia.

REFERENCES

1. Xu, H.; Chen, R.; Sun, Q.; Lai,W.; Su, Q.; Huang, W.; Liu, X. Recent Progress in Metal–Organic Complexes for Optoelectronic Applications. *Coord. Chem. Rev.*, **2014**, *43*, 3259-3302.
2. Xiao, L.; Chen, Z.;Qu, B.;Luo, J.; Kong, S.;Gong,Q.; J. Kido. Recent Progresses on Materials for Electrophosphorescent Organic Light-Emitting Devices. *Adv. Mater.*, **2011**, *23*, 926-952.
3. Chi, Y.; Chou, P. T. Transition-Metal Phosphors with Cyclometalating Ligands: Fundamentals and Applications. *Chem. Soc. Rev.*, **2010**, *39*, 638-655.
4. Tang, M.-C.; Chan, A. K.-W.; Chan, M.-Y.; Yam, V. W.-W. Platinum and Gold Complexes for OLEDs**.** *Top Curr. Chem.*, **2016**, 374:46.
5. Yu, T.; Tsang, D. P.-K.; Au, V. K.-M.; Lam, W. H.; Chan, M.-Y.; Yam,V. W.-W. Deep Red to Near-Infrared Emitting Rhenium(I) Complexes: Synthesis, Characterization, Electrochemistry, Photophysics, and Electroluminescence Studies. *Chem. Eur. J.*, **2013**, *19*, 13418 – 13427.
6. Yersin, H. Triplet Emitters for OLED Applications.Mechanisms of Exciton Trapping and Control of Emission Properties**.** *Top. Curr. Chem.,* **2004**, *241*, 1-26.

7. Yersin, H.; Rausch, A. F.; Czerwieniec, R.; Hofbeck,T.; Fischer,T. The Triplet State of Organo-Transition Metal Compounds. Triplet Harvesting and Singlet Harvesting for Efficient OLEDs. *Coord. Chem. Rev.*, **2011**, *255*, 2622-2652.

8. Williams, J. A. G. *In Photochemistry and Photophysics of Coordination Compounds II* Springer Berlin Heidelberg, Berlin, Heidelberg, 2007.

9. Li, K.; Tong, G. S. M.; Wan, Q.; Cheng, G.; Tong, W.-Y.; Ang, W.-H.; Kwong, W.-L.; Che, C.-M. Highly Phosphorescent Platinum(II) Emitters: Photophysics, Materials and Biological Applications. *Chem. Sci.*, **2016**, *7*, 1653-1873.

10. Li, K.; Guan, X.; Ma, C.-W.; Lu, W.; Chen, Y.; Che, C.-M. Blue Electrophosphorescent Organoplatinum(II) Complexes with Dianionic Tetradentate Bis(carbene) Ligands. *Chem. Commun.*, **2011**, *47*, 9075-9077.

11. Li, K.; Chen, Y.; Lu, W.; Zhu, N.; Che C.-M. A Cyclometalated Platinum(II) Complex with a Pendent Pyridyl Motif as Solid-State Luminescent Sensor for Acidic Vapors. *Chem. Eur. J.*, **2011**, *17*, 4109 - 4112.

12. Li, K.; Cheng, G.; Ma, C.; Guan, X.; Kwok, W.-M.; Chen, Y.; Lu, W.; Che, C.-M. Light-Emitting Platinum(II) Complexes Supported by Tetradentate Dianionic bis(N-Heterocyclic Carbene) Ligands: towards Robust Blue Electrophosphors. *Chem. Sci.*, **2013**, *4*, 2630-2644.

13. Zhang, Y.; Garg, J. A.; Michelin, C.; Fox, T.; Blacque, O.; Venkatesan. K. Synthesis and Luminescent Properties of cis Bis-N-Heterocyclic Carbene Platinum(II) Bis-Arylacetylide Complexes. *Inorg. Chem.*, **2011**, *50*, 1220-1228.

14. Zhang, Y.; Clavadetscher, J.; Bachmann, M.; Blacque, O.; Venkatesan. K. Tuning the Luminescent Properties of Pt(II) Acetylide Complexes through Varying the Electronic Properties of N-Heterocyclic Carbene Ligands. *Inorg. Chem.*, **2014**, *53*, 756−771.

15. Bachmann, M.; Suter, D.; Blacque, O.; Venkatesan. K. Tunable and Efficient White Light Phosphorescent Emission Based on Single Component N-Heterocyclic Carbene Platinum(II) Complexes. *Inorg. Chem.*, **2016**, *55*, 4733−4745.

16. Leopold, H.; Heinemeyer, U.; Wagenblast, G.; Münster. I.; Strassner, T.. Changing the Emission Properties of Phosphorescent C^C*-Cyclometalated Thiazol-2-ylidene Platinum(II) Complexes by Variation of the b-Diketonate Ligands. *Chem. Eur. J.* **2016**, *22*, 1 – 12 and references therein.

17. Rausch, A. F.; Murphy, L.; Williams J. A. G.; Yersin, H. Improving the Performance of Pt(II) Complexes for Blue Light Emission by Enhancing the Molecular Rigidity. *Inorg. Chem.*, **2011**, *51*, 312-319.

18. Brooks, J.; Babayan, Y.; Lamansky, S.; Djurovich, P. I.; Tsyba, I.; Bau, R. T.; Thompson, M. E. Synthesis and Characterization of Phosphorescent Cyclometalated Platinum Complexes. *Inorg. Chem.*, **2002**, *41*, 3055-3066.

19. Huo, S.; Carroll, J.; Vezzu, D. A. K. Design, Synthesis, and Applications of Highly Phosphorescent Cyclometalated Platinum Complexes. *Asian J. Org. Chem.*, **2015**, *4*, 1210-1245.

20. Williams, J. A. G.; Beeby, A.; Davies, E. S.; Weinstein, J. A.; Wilson, C. An Alternative Route to Highly Luminescent Platinum(II) Complexes: Cyclometalation with N^C^N-Coordinating Dipyridylbenzene Ligands. *Inorg. Chem.*, **2003**, *42*, 8609-8611.

21. Feng, K.; Zuniga, C.; Zhang, Y.-D.; Kim, D.; Barlow, S.; Marder, S. R.; Brédas, J. L.; Weck, M. Norbornene-Based Copolymers Containing Platinum Complexes and Bis(carbazolyl)benzene Groups in Their Side-Chains. *Macromelecules*, **2009**, *42*, 6855-6864.

22. Kui, S. C. F.; Chow, P. K.; Tong, G. S. M.; Lai, S.-L.; Cheng, G.; Kwok, C.-C.; Low, K.-H.; Ko, M. Y.; Che, C.-M. Robust Phosphorescent Platinum(II) Complexes Containing Tetradentate O^N^C^N Ligands: Excimeric Excited State and Application in Organic White-Light-Emitting Diodes. *Chem. -Eur. J.*, **2013**, *19*, 69-73.

23. Hang, X.-C.; Fleetham, T.; Turner, E.; Brooks, J.; Li, J. Highly Efficient Blue-Emitting Cyclometalated Platinum(II) Complexes by Judicious Molecular Design. *Angew. Chem., Int. Ed.*, **2013**, *52*, 6753-6756.

24. Turner, E.; Bakken, N.; Li, J. Cyclometalated Platinum Complexes with Luminescent Quantum Yields Approaching 100%. *Inorg. Chem.*, **2013**, *52*, 7344-7351.

25. Tronnier, A.; Wagenblast, G.; Münster, I.; Strassner, T. Phosphorescent Platinum(II) Complexes with C^C* Cyclometalated NHC Dibenzofuranyl Ligands: Impact of Different Binding Modes on the Decay Time of the Excited State. *Chem. Eur. J.*, **2015**, *21*, 12881-12884 and references therein.

26. Hudson, Z. M.; Sun, C.; Helander, M. G.; Chang, Y. L.; Lu Z. H.; Wang, S. N. Highly Efficient Blue Phosphorescence from Triarylboron-Functionalized Platinum(II) Complexes of N-Heterocyclic Carbenes. *J. Am. Chem. Soc.*, **2012**, *134*, 13930-13933.

27. Tronnier, A.; Nischan, N.; Metz, S.; Wagenblast, G.; Münster, I.; Strassner, T. Phosphorescent C^C* Cyclometalated Pt^{II} Dibenzofuranyl-NHC Complexes – An Auxiliary Ligand Study. *Eur. J. Inorg. Chem.*, **2014**, *2014*, 256-264.

28. Tronnier, A.; Metz, S.; Wagenblast, G.; Münster, I.; Strassner, T. Blue phosphorescent nitrile containing C^C* cyclometalated NHC platinum(II) complexes. *Dalton Trans.*, **2014**, *43*, 3297-3305.

29. Tronnier, A.; Risler, A.; Langer, N.; Wagenblast, G.; Münster, I.; Strassner, T. A Phosphorescent C^C* Cyclometalated Platinum(II)Dibenzothiophene NHC Complex. *Organometallics*, **2012**, *31*, 7447-7452.

30. Unger, Y.; Meyer, D.; Molt, O.; Schildknecht, C.; Münster, I.; Wagenblast, G.; Strassner, T. Green–Blue Emitters: NHC-Based Cyclometalated [Pt(C^C*)(acac)] Complexes. *Angew. Chem., Int. Ed.*, **2010**, *49*, 10214-10216.

31. Tronnier, A.; Pöthig, A.; Metz, S.; Wagenblast, G.; Münster, I.; Strassner, T. Enlarging the π System of Phosphorescent (C^C*) Cyclometalated Platinum(II) NHC Complexes. *Inorg. Chem.*, **2014**, *53*, 6346-6356.

32. Tenne, M.; Metz, S.; Wagenblast, G.; Münster, I.; Strassner, T. C^C* Cyclometalated Platinum(II) N-Heterocyclic Carbene Complexes with a Sterically Demanding β-Diketonato Ligand – Synthesis, Characterization and Photophysical Properties. *Dalton Trans.*, **2015**, *44*, 8444-8455.

33. Fuertes, S.; Garcia, H.; Peralvarez, M.; Hertog, W.; Carreras, J.; Sicilia, V. Stepwise Strategy to Cyclometallated Pt^{II} Complexes with N-Heterocyclic Carbene Ligands: A Luminescence Study on New β-Diketonate Complexes. *Chem. - Eur. J.*, **2015**, *21*, 1620-1631.

34. Ko, S.-B.; Park, H.-J.; Gong, S.; Wang, X. N.; Lu, Z.-H.; Wang, S. N. Blue Phosphorescent N-Heterocyclic Carbene Chelated Pt(II) Complexes with an α-Duryl-β-Diketonato Ancillary Ligand. *Dalton Trans.*, **2015**, *44*, 8433-8443.

35. Fuertes, S.; Chueca, A. J.; Perálvarez, M.; Borja, P.; Torrell, M.; Carreras, J.; Sicilia,V. White Light Emission from Planar Remote Phosphor Based on NHC Cycloplatinated Complexes. *ACS App. Mat. Interfaces*, **2016**, *8*, 16160-16169.

36. Fuertes, S.; Chueca, A. J.; Sicilia, V. Exploring the Transphobia Effect on Heteroleptic NHC Cycloplatinated Complexes. *Inorg. Chem.*, **2015**, *54*, 9885-9895.

37. Lu, W.; Mi, B.-X.; Chan, M. C. W.; Hui, Z.; Che, C.-M.; Zhu, N.; Lee, S.-T. Light-Emitting Tridentate Cyclometalated Platinum(II) Complexes Containing σ-Alkynyl Auxiliaries: Tuning of Photo- and Electrophosphorescence. *J. Am. Chem. Soc.*, **2004**, *126*, 4958-4971.

38. Kavitha, J.; Chang, S.-Y.; Chi, Y.; Yu, J.-K.; Hu, Y.-H.; Chou, P.-T.; Peng, S.-M.; Lee, G.-H.; Tao, Y.-T.; Chien, C.-H.; Carty, A. J. In Search of High-Performance Platinum(II) Phosphorescent Materials for the Fabrication of Red Electroluminescent Devices. *Adv. Funct. Mater.*, **2005**, *15*, 223-229.

39. Mydlak, M.; Mauro, M.; Polo, F.; Felicetti, M.; Leonhardt, J.; Diener, G.; De Cola, L.; Strassert, C. A. Controlling Aggregation in Highly Emissive Pt(II) Complexes Bearing Tridentate Dianionic N^N^N Ligands. Synthesis, Photophysics, and Electroluminescence. *Chem. Mater.*, **2011**, *23*, 3659-3667.

40. Cebrián, C.; Mauro, M.; Kourkoulos, D.; Mercandelli, P.; Hertel, D.; Meerholz, K.; Strassert, C. A.; De Cola, L. Luminescent Neutral Platinum Complexes Bearing an Asymmetric N^N^N Ligand for High-Performance Solution-Processed OLEDs. *Adv. Mater.*, **2013**, *25*, 437-442.

41. Cheng, G.; Chow, P.-K.; Kui, S. C. F.; Kwok, C.-C.; Che, C.-M. Light-Emitting Devices: High-Efficiency Polymer Light-Emitting Devices with Robust Phosphorescent Platinum(II) Emitters Containing Tetradentate Dianionic O^N^C^N Ligands. *Adv. Mater.*, **2013**, *25*, 6765-6770

42. Li, H.; Li, J.; Ding, J.; Yuan, W.; Zhang, Z.; Zou, L.; Wang, X.; Zhan, H.; Xie, Z.; Cheng, Y.; Wang, L. Design, Synthesis, and Optoelectronic Properties of Dendrimeric Pt(II) Complexes and Their Ability to Inhibit Intermolecular Interaction. *Inorg. Chem.* **2014**, *53*, 810-821.

43. Mróz, W.; Botta, C.; Giovanella, U.; Rossi, E.; Colombo, A.; Dragonetti, C.; Roberto, D.; Ugo, R.; Valore, A.; Williams, J. A. G. Cyclometallated Platinum(II) Complexes of 1,3-di(2-pyridyl)benzenes for Solution-Processable WOLEDs Exploiting Monomer and Excimer Phosphorescence. *J. Mater. Chem.*, **2011**, *21*, 8653-8661.

44. Li, H.; Ding, J.; Xie, Z.; Cheng, Y.; Wang, L. Synthesis, Characterization and Electrophosphorescent Properties of Mononuclear Platinum(II) Complexes Based on 2-Phenylbenzoimidazole Derivatives. *J. Organomet. Chem.*, **2009**, *694*, 2777-2785.

45. Kong, F. K.-W.; Tang, M.-C.; Wong, Y.-C.; Chan, M.-Y.; Yam, V. W.-W. Design Strategy for High-Performance Dendritic Carbazole-Containing Alkynylplatinum(II) Complexes and Their Application in Solution-Processable Organic Light-Emitting Devices. *J. Am. Chem. Soc.*, **2016**, *138*, 6281-6291.

46. Li, H.; Yuan, W.; Wang, X.; Zhan, H.; Xie, Z.; Cheng, Y. Enhancement of Luminescence Performance from the Alteration of Stacking Patterns of Pt(II) Dendrimers. *J. Mater. Chem. C*, **2015**, *3*, 2744-2750.

47. Hsu, C.-W.; Ly, K. T.; Lee, W.-K.; Wu, C.-C.; Wu, L.-C.; Lee, J.-J.; Lin, T.-C.; Liu, S.-H.; Chou, P.-T.; Lee, G.-H.; Chi, Y. Triboluminescence and Metal Phosphor for Organic Light-Emitting Diodes: Functional Pt(II) Complexes with Both 2-Pyridylimidazol-2-ylidene and Bipyrazolate Chelates. *ACS Appl. Mater. Interfaces* **2016**, *8*, 33888-33898.

48. Tseng, C.-H.; Fox, M. A.; Liao, J.-L.; Ku, C.-H.; Sie, Z.-T.; Chang, C.-H.; Wang, J.-Y.; Chen, Z.-N.; Lee, G.-H.; Chi, Y. Luminescent Pt(II) Complexes Featuring Imidazolylidene–Pyridylidene and Dianionic Bipyrazolate: from Fundamentals to OLED Fabrications. *J. Mater. Chem. C*, **2017**, *5*, 1420-1435.

49. Mabbott, D. J.; Mann, B. E.; Maitlis, P. M. Cationic (η^3-allylic)(η^4-diene)-Palladium and -Platinum Complexes. *J. Chem. Soc., Dalton Trans.*, **1977**, 294-299.

50. Zucca, A.; Maidich, L.; Carta, V.; Petretto, G. L.; Stoccoro, S.; Cinellu, M. A.; Pilo, M. I.; Clarkson, G. J. Cyclometalated Complexes of Platinum(II) with 2-Vinylpyridine. *Eur. J. Inorg. Chem.*, **2014**, *2014*, 2278-2287.

51. Maidich, L.; Zuri, G.; Stoccoro, S.; Cinellu, M. A.; Zucca, A. Assembly of Symmetrical and Unsymmetrical Platinum(II) Rollover Complexes with Bidentate Phosphine Ligands. *Dalton Trans.*, **2014**, *43*, 14806-14815.

52. Minghetti, G.; Zucca, A.; Stoccoro, S.; Cinellu, M. A.; Manassero, M.; Sansoni, M. Six-Membered Cyclometallated Derivatives of Platinum(II) Derived from 2-Benzylpyridines. Crystal and Molecular Structure of [Pt(L)(Ph_3P)Cl] (HL = 2-(1-methylbenzyl)pyridine). *J. Organomet. Chem.*, **1994**, *481*, 195-204.

53. Vicente, J.; Abad, J. A.; Martinez-Viviente, E.; Jones, P. G.. Study of the Reactivity of 2-Acetyl-, 2-Cyano-, 2-Formyl-, and 2-Vinylphenyl Palladium(II) Complexes. Mono- and Triinsertion of an Isocyanide into the Pd−C Bond. A 2-Cyanophenyl Palladium Complex as a Ligand. *Organometallics*, **2002**, *21*, 4454-4467.

54. Vicente, J.; Abad, J. A.; Hernández-Mata, F. S.; Jones, P. G. An Unusual Palladium Complex Involved in an Unusual Rearrangement of Ortho-palladated Aryldithioacetals. *J. Am. Chem. Soc.*, **2002**, *124*, 3848-3849.

55. Vicente, J.; Arcas, A.; Gálvez-López, M. D.; Jones, P. G. Bis(2,6-initroaryl)platinum(II) Complexes. Cis/Trans Isomerization. *Organometallics* **2006**, *25*, 4247-4259.

56. Casas, J. M.; Fornies, J.; Fuertes, S.; Martin, A.; Sicilia, V.. New Mono- and Polynuclear Alkynyl Complexes Containing Phenylacetylide as Terminal or Bridging Ligand. X-ray Structures of the Compounds $NBu_4[Pt(CH_2C_6H_4P(o\text{-}tolyl)_2\text{-}\kappa C,P)(C{\equiv}CPh)_2]$, $[Pt(CH_2C_6H_4P(o\text{-}tolyl)_2\text{-}\kappa C,P)(C{\equiv}CPh)(CO)]$, $[\{Pt(CH_2C_6H_4P(o\text{-}tolyl)_2\text{-}\kappa C,P)(\mu\text{-}C{\equiv}CPh)\}_2]$, and $[\{Pt(CH_2C_6H_4P(o\text{-}tolyl)_2\text{-}\kappa C,P)(C{\equiv}CPh)_2Cu\}_2]$. *Organometallics*, **2007**, *26*, 1674-1685.

57. Sicilia, V.; Fuertes, S.; Martin, A.; Palacios, A. N-Assisted CPh–H Activation in 3,8-Dinitro-6-phenylphenanthridine. New C,N-Cyclometalated Compounds of Platinum(II): Synthesis, Structure, and Luminescence Studies. *Organometallics*, **2013**, *32*, 4092-4102.

58. Tronnier, A.; Pöthig, A.; Herdtweck, E.; Strassner, T. C^C* Cyclometalated Platinum(II) NHC Complexes with β-Ketoimine Ligands. *Organometallics*, **2014**, 33, 898-908.

59. Tronnier, A.; Nischan N.; Strassner, T. Cˆ C*-Cyclometalated Platinum(II) Complexes with Trifluoromethyl-Acetylacetonate Ligands – Synthesis and Electronic Effects. *J. Organomet. Chem.*, **2013**, *730*, 37-43.

60. Hudson, Z. M.; Blight, B. A.; Wang, S. N. Efficient and High Yield One-Pot Synthesis of Cyclometalated Platinum(II) beta-Diketonates at Ambient Temperature. *Org. Lett.*, **2012**, *14*, 1700-1703.

61. Rao, Y.-L.; Wang, S. N. Impact of Constitutional Isomers of $(BMes_2)$phenylpyridine on Structure, Stability, Phosphorescence, and Lewis Acidity of Mononuclear and Dinuclear Pt(II) Complexes. *Inorg. Chem.*, **2009**, 48, 7698-7713.

62. Harris, C. F.; Vezzu, D. A. K.; Bartolotti, L.; Boyle, P. D.; Huo, S. Q. Synthesis, Structure, Photophysics, and a DFT Study of Phosphorescent C*N^N- and C^N^N-Coordinated Platinum Complexes. *Inorg. Chem.*,**2013**, *52*, 11711-11722.

63. Karakostas, N.; Mavridis, I. M.; Seintis, K.; Fakis, M.; Koini, E. N.; Petsalakis, I. D.; Pistolis, G. Highly Efficient and Unidirectional Energy Transfer within a Tightly Self-Assembled Host-Guest Multichromophoric Array. *Chem. Commun.*, **2014**, *50*, 1362-1365.

64. Jude, H.; Bauer, J. A. K.; Connick, W. B. Tuning the Electronic Structures of Platinum(II) Complexes with a Cyclometalating Aryldiamine Ligand. *Inorg. Chem.*, **2004**, *43*, 725-733.

65. Crespo, M.; Anderson, C. M.; Kfoury, N.; Font-Bardia, M.; Calvet, T. Reductive Elimination from Cyclometalated Platinum(IV) Complexes To Form Csp2–Csp3 Bonds and Subsequent Competition between Csp2–H and Csp3–H Bond Activation. *Organometallics*, **2012**, *31*, 4401-4404.

66. Alcarazo, M.; Radkowski, K.; Goddard, R.; Furstner, A. Metal Complexes with Carbene Ligands Stabilized by Lateral Enamines. *Chem. Commun.*, **2011**, *47*, 776-778.

67. Anderson, C.; Crespo, M.; Rochon, F. D. Stereoselective Oxidative Addition of Methyl Iodide to Chiral Cyclometallated Platinum(II) Compounds Derived from (R)-(+)-1-(1-naphthylethylamine). Crystal Structure of [67]. *J. Organomet. Chem.*, **2001**, *631*, 164-174.

68. Rodríguez, J.; Zafrilla, J.; Albert, J.; Crespo, M.; Granell, J.; Calvet, T.; Font-Bardia, M. Cyclometallated Platinum(II) Compounds with Imine Ligands Derived from Amino Acids: Synthesis and Oxidative Addition Reactions. *Organomet. Chem.*, **2009**, *694*, 2467-2475.

69. Diez, A.; Fornies, J.; Fuertes, S.; Lalinde, E.; Larraz, C.; Lopez, J. A.; Martin, A.; Moreno, M. T.; Sicilia, V. Synthesis and Luminescence of Cyclometalated Compounds with Nitrile and Isocyanide Ligands. *Organometallics*, **2009**, *28*, 1705-1718.

70. Graber, S.; Doyle, K.; Neuburger, M.; Housecroft, C. E.; Constable, E. C.; Costa, R. D.; Orti, E.; Repetto, D.; Bolink, H. J. A Supramolecularly-Caged Ionic Iridium(III) Complex Yielding Bright and Very Stable Solid-State Light-Emitting Electrochemical Cells. *J. Am. Chem. Soc.*, **2008**, *130*, 14944-14945.

71. Jude, H.; Rein, F. N.; White, P. S.; Dattelbaum, D. M.; Rocha, R. C. Synthesis, Structure, and Electronic Properties of a Dimer of Ru(bpy)(2) Doubly Bridged by Methoxide and Pyrazolate. *Inorg. Chem.*, **2008**, *47*, 7695-7702.

72. Williams, J. A. G. Photochemistry and Photophysics of Coordination Compounds: Platinum. *Top. Curr. Chem.*, **2007**, *281*, 205-268.

73. Soellner, J.; Tenne, M.; Wagenblast, G.; Strassner, T. Phosphorescent Platinum(II) Complexes with Mesoionic 1*H*-1,2,3-Triazolylidene Ligands. *Chem. Eur. J.*, **2016**, *22*, 9914-9918.

74. Giovanella, U.; Betti, P.; Botta, C.; Destri, S.; Moreau, J.; Pasini, M.; Porzio, W.; Vercelli, B.; Bolognesi, A. All-Conjugated Diblock Copolymer Approach to Improve Single Layer Green Electroluminescent Devices. *Chem. Mater.*, **2011**, *23*, 810-816.

Table of Contents Synopsis

The heteroleptic compounds $[Pt(R\text{-}C\text{^}C^*)(PPh_3)L]PF_6$ (R-C = Naph, R = CO_2Et, L = py; R = CN; L = py, CNXyl, MMI), were selectively obtained as the trans-(C*, PPh_3) isomer. They are efficient blue- or greenish-blue Pt(II) emitters in PMMA films, with QY values ranging from 68% to 93%. Electroluminescent devices with blue (**2C**), yellow-orange (**3C**) and white light (mixtures of **2C:3C**) emissions were fabricated by a full solution process technology with a non-doped emitting layer.

“For Table of Contents Only”